(Light) Stop Signs

Preprint typeset in JHEP style - HYPER VERSION

(Light) Stop Signs

Zhenyu Han, Andrey Katz, David Krohn, and Matthew Reece

Department of Physics, Harvard University, Cambridge, MA 02138
E-mail: zhan,andrey,dkrohn,mreece@physics.harvard.edu

Abstract: Stop squarks with a mass just above the top's and which decay to a nearly massless LSP are difficult to probe because of the large SM di-top background. Here we discuss search strategies which could be used to set more stringent bounds in this difficult region. In particular, we note that both the rapidity difference $\Delta y(t, \bar{t})$ and spin correlations (inferred from, for example, $\Delta\phi(\ell^+, \ell^-)$) are sensitive to the presence of stops. We emphasize that systematic uncertainties in top quark production can confound analyses looking for stops, making theoretical and experimental progress on the understanding of Standard Model top production at high precision a very important task. We estimate that spin correlation alone, which is relatively robust against such systematic uncertainties, can exclude a 200 GeV stop at 95% confidence with 20 fb^{-1} at the 8 TeV LHC.

Contents

1. Introduction

Supersymmetry remains the most compelling theoretical explanation for how the vast hierarchy between weak and Planck scales can persist in the face of quantum mechanical effects. The leading quantum corrections that make the Standard Model an unnatural theory are the quadratically divergent contributions of top quark loops to the Higgs boson mass term, which are largely canceled in supersymmetric theories by loops of scalar tops. Minimizing fine tuning in supersymmetric theories, then, requires that the stop mass be as close to the top mass as possible. From the theoretical viewpoint, this motivates consideration of models in which the stop may be among the lightest superpartners [1, 2].

The LHC is setting ever more stringent bounds on SUSY. Very roughly, if the first and second generation squarks are all of the same mass and they decay as $\tilde{q} \to q + \chi^0$ the current bounds require $m_{\tilde{q}} \gtrsim 1.3$ TeV (for decoupled gluinos), and if the gluinos decay as $\tilde{g} \to q\bar{q}+\chi^0$ the bound is roughly $m_{\tilde{g}} \gtrsim 1$ TeV (for decoupled squarks). These bounds come primarily from searches for jets + MET [3, 4, 5, 6], and become stronger if squarks and gluinos have comparable masses. These results force "vanilla" supersymmetry, meaning the class of well-studied models with flavor universal squark masses and large amounts of missing transverse momentum in decays, into an uncomfortably unnatural corner.

However, current data allows another interesting possibility. If squarks of the third generation are significantly lighter than those of the first two, the bounds on the lighter particles can be considerably weaker [7, 8, 9, 10, 11, 12]. Sbottoms which decay as $\tilde{b} \to b + \chi^0$, for instance, are only constrained to $m_{\tilde{b}} \gtrsim 400$ GeV for light LSPs, with the bounds becoming much less stringent as m_{χ^0} is increased [13]. Perhaps the weakest bounds are on the stop, which after 1 fb^{-1} is still allowed to be at or perhaps slightly below the top mass, according to theoretical estimates [14, 8] that carry too much uncertainty in detector modeling to make a sharp claim. Third generation squarks produced indirectly in gluino decays lead to signatures of same-sign dileptons or of jets and MET, constraining the gluino to be heavier than about 850 to 950 GeV [15, 16, 17, 18], which is still compatible with naturalness.[1]

These considerations strongly motivate a deeper study of the phenomenology of light stops. The study of simplified spectra, based on naturalness considerations, in which a stop decays to a top and neutralino was advocated in [26], and a number of related works have appeared since [27, 28, 29, 30], as well as variations in which the stop plays a role in coannihilation to explain dark matter abundance [31, 32] or has flavor-violating couplings to explain top A_{FB} [33]. (We have recently learned of two other papers in preparation [34, 35] that take different approaches to the problem, which may be complementary to ours.) The challenge of stop phenomenology is to disentangle the stop signal from top backgrounds. For our purposes, it is useful to introduce a division of $\tilde{t} \to bW^+\chi^0$ signals into three categories depending on the stop mass:

- *Three-body stops*: if stops are light enough, they cannot decay to an on-shell top quark and a neutralino (or gravitino), so the three-body decay $\tilde{t} \to bW^+\chi^0$ dominates. (With more extreme squeezing of the spectrum, a four-body decay or flavor-violating decay may result, but we will not consider this limit.) Many kinematic distributions such as $m_{\ell b}$ or transverse mass for stop decay will be significantly different from those in top decay [36, 14]. However, this region also suffers from relatively low acceptance, and probably deserves a closer look in the future.

- *Two-body stops*: if $m_{\tilde{t}} \gg m_t$, the decay is two-body, $\tilde{t} \to t\chi^0$, and the invisible neutralino or gravitino can carry away a large amount of momentum. The simplest way to exploit this is to impose a hard MET cut. More sophisticated approaches use the fact that MET in the top background arises from neutrinos in W decay, which suggests the power of a transverse mass cut in the semileptonic case [27] and a cut on M_{T2} computed with the two leptons and MET in the dileptonic case [37, 8]. A recent update on this regime appeared in Ref. [38].

- *Stealth ("one-body") stops*: if the neutralino (or gravitino) is light and $m_{\tilde{t}}$ is only slightly larger than m_t, two-body decays $\tilde{t} \to t\chi^0$ in which the momentum of χ^0 is very small can predominate. Kinematically, these are effectively "one-body decays" since the top carries all the momentum, and stop pair production can be extremely

[1] For theoretical models which motivate a closer look at SUSY with light third generation superpartners see e.g. [19, 20, 21, 22, 23, 24, 25].

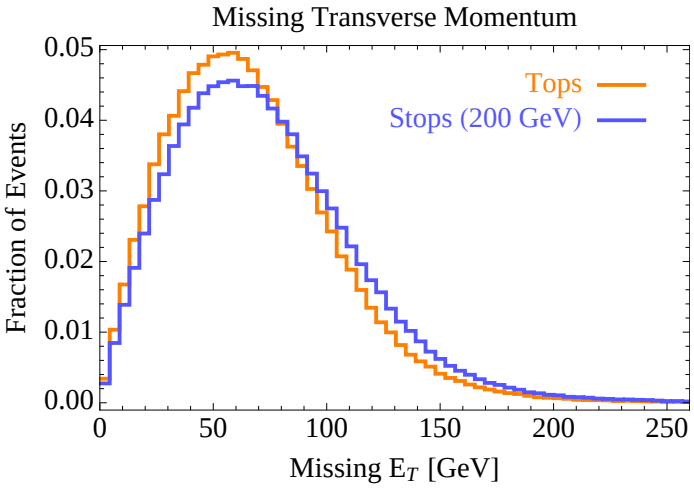

Figure 1: $\not{E}_{\rm T}$ distribution in top and stop events, where we have considered stop decays to massless neutralinos. The rate is normalized to the number of events with two isolated leptons.

difficult to separate from top pair production [39]. Furthermore, unlike compressed supersymmetry scenarios, the events do not become more distinctive when recoiling against an additional hard jet [40].

The stealth stop regime is the most challenging and can involve a large new physics cross section at the LHC. This regime is the focus of our current study.

We illustrate the stealth regime in Fig. 1, which shows the missing transverse energy distribution for dileptonic events from top pairs and 200 GeV stop pairs (decaying as $\tilde{t} \to t\chi^0$). This is based on a simulation with cuts that we will describe in Sec. 4.3. The distributions for tops and stops are very similar, because in the rest frame of the stop, in the limit of small mass difference and massless χ^0, the momentum of the decay products is $\approx \delta m = m_{\tilde{t}} - m_t$. In the lab frame, the χ^0 carries away invisible momentum of order $\gamma\ \delta m$, and for production of typical stop pairs the boost is not large.

If a stop decays to a massless neutralino, the transition from the three-body regime to the stealth regime is not smooth. The three-body decay ends abruptly at $m_{\tilde{t}} = m_t$, at which point two-body stealth decays dominate until the mass splitting becomes large enough that the decays are no longer stealthy. The case of a stop decay to a gravitino is slightly more subtle; the gravitino couples to SUSY breaking, leading to two extra powers of $m_{\tilde{t}} - m_t$ phase-space suppression in the two-body decay rate. This allows the three-body regime to extend to somewhat higher masses, as illustrated in Fig. 2. (This plot and others throughout the paper rely on simulations performed with MadGraph 5 [41], as well as goldstino vertices we have implemented [42] using the UFO format [43]). The estimates in [8] show that current analyses have weakened sensitivity in the range $m_t \lesssim m_{\tilde{t}} \lesssim 250$ GeV, which we will take as our characterization of the stealth stop window. We review the current searches relevant for stops in Sec. 2, characterizing the extent to which they are simple top rate measurements in this window. Although more data will reduce the statistical errors on measurements of the top, both experimental systematics

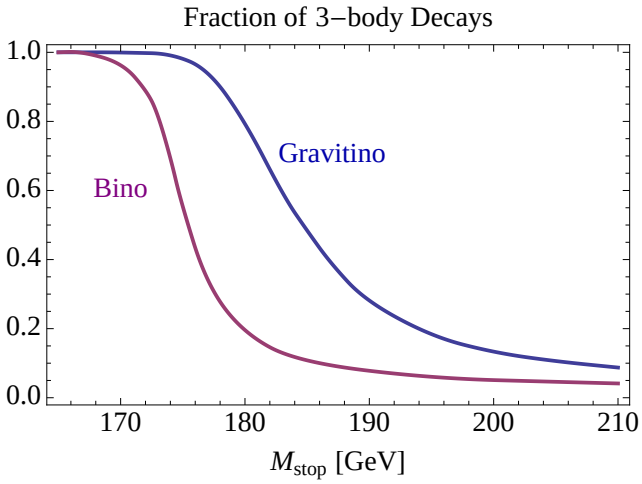

Figure 2: Fraction of stop decays, $\tilde{t} \to W^+ b\chi$, which are three-body, as a function of the stop mass. More precisely, we are labeling a decay "three-body" when $m(W^+b) < m_t - 3\Gamma_t$, and have taken the top quark mass to be 173 GeV. The neutral fermion χ is either the gravitino $\tilde{G}$ or a massless bino $\tilde{B}$. In the gravitino case, three-body decays persist for larger stop masses, so the "maximally stealthy stop" is at masses nearer 200 GeV than 175 GeV.

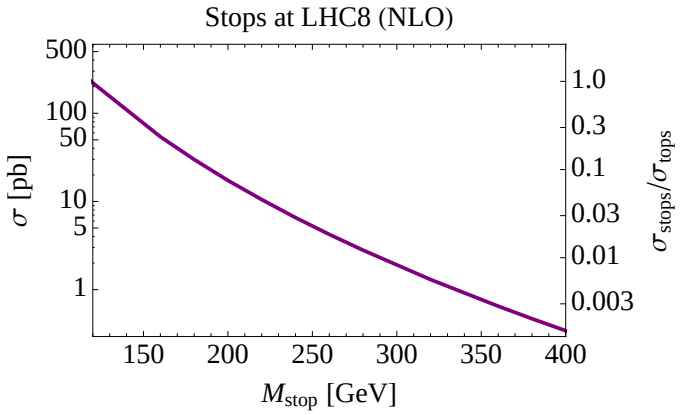

Figure 3: NLO stop pair production cross section at the 8 TeV LHC, as reported by Prospino [45]. The vertical axis on the right shows the rate as a ratio to the $t\bar{t}$ rate.

and theoretical uncertainties will remain. Measurements of the top are notoriously difficult (see, e.g., Ref. [44]), and so the more handles one has to constrain/discover stops, the better.

Here we present a set of search strategies which can be used to constrain stops in this difficult region of parameter space. While we find no single smoking-gun signature for light stops, a few robust physical considerations can enhance the sensitivity of searches. It will be important to combine these considerations, because stops are rare. At the 7 TeV LHC, the top cross section is about 165 pb (increasing to about 230 pb with 8 TeV collisions [46]), while the stop cross section for $m_{\tilde{t}} = m_t$ is only about one-sixth as large, and drops steeply at larger masses. (See Fig. 3 for NLO results; recent, more accurate, calculations of stop production may be found in [47].) Thus, finding stops by simply measuring the total rate

Observable	Feasibility
Top production rate	Stops near m_t can increase the measured value of $\sigma_{t\bar{t}}$ by up to $\sim 15\%$. However, (1) even at NNLL the uncertainties in $\sigma_{t\bar{t}}$ are $\sim 10\%$ and (2) theoretical ambiguities in the interpretation of the measured value of m_t can further increase the uncertainty by a similar degree.
$\not{E}_{\rm T}$-based quantities	While the LSP from stop decays contributes to the $\not{E}_{\rm T}$ in an event, this effect is usually greatly diluted by the contributions from neutrinos (again, for $m_{\tilde{t}}$ near m_t). When this is not the case (*e.g.*, with fully-hadronic top decays, or in the tails of m_T distributions) we expect the experimental systematics to be very challenging.
$\Delta y(t,\bar{t})$	The shape of the $\Delta y(t,\bar{t})$ distribution differs markedly between stop and top production. However, once one accounts for the small stop production rate this effect can be mimicked by QCD NLO uncertainties.
Spin correlations	Measurements of top spin correlation at the LHC are quite insensitive to higher order corrections, and show a clear difference between top and stop production. While we expect this measurement to be statistically limited, we conclude that this is one of the most robust channels to use in searching for light stops.

Table 1: A summary of observables sensitive to the presence of stops above the SM di-top background, and comments on the feasibility of employing these in searching for light stops. Note that when we speak of tops in stop events we are referring to stops reconstructed as tops.

of events passing top selection cuts is a challenge.

The most important physical handle on stops in the stealthy regime is the characteristic that allows them to play their divergence-canceling role in SUSY: they are bosons, not fermions. In particular, because they are spin zero, they are produced without spin correlations and the decay of a stop and antistop are completely uncorrelated. Top pair production, on the other hand, involves spin correlation effects, linking the decay angles on the two sides of the event. Thus, a top pair sample enriched by stealthy stops should have correlations that are washed out by an amount related to the stop cross section. The effect is small, but it still can be used, and we elaborate on these ideas in Sec. 3. Even more important, it was shown in [48] that full matrix element spin-correlation measurement is stable with respect to NLO corrections, suffering from very mild systematic uncertainties. Stability with respect to NLO corrections distinguishes this measurement from other methods.

Other effects that we use to discriminate between these two samples have to do with smallness of $\tilde{t}\bar{\tilde{t}}$ production compared to $t\bar{t}$. Two effects conspire to suppress the production rate of stops compared to tops near the threshold. First, the process $gg \to t\bar{t}$ has t- and u-channel singularities, which are regularized by m_t. There is no analogous singularity in $\tilde{t}\tilde{t}^*$ production; therefore $t\bar{t}$ production is enhanced, and $t\bar{t}$ events tend to have larger rapidity gap between tops, relative to $\tilde{t}\tilde{t}^*$. This is the most important stop rate suppression mechanism at the LHC. On the other hand, one can take advantage of the rapidity gap as a possible discriminator. We will elaborate on this potentially useful handle in sec-

tion 4, though we notice that this approach can suffer from unpleasantly large systematic uncertainties. Another mechanism which suppresses the stop production rate is a p-wave suppression in the s-channel stop production from a $q\bar{q}$ initial state, motivating a look at the higher p_T regime, where the stop portion in the sample might be enhanced. This process is very important at the Tevatron, but less interesting at the LHC due to suppressed $q\bar{q}$ parton luminosities. We will further comment on this in Appendix B. Although we do not show a single channel allowing for stealthy stop discovery, we claim that a combination of the above mentioned tools can give us more than 2σ sensitivity to a stealthy stop by the end of $\sqrt{s} = 8$ TeV run. We summarize the expected sensitivity in Table 1.

Our paper is organized as follows. In the next section we review the current searches for SUSY and further discuss the features of the stealth regime. In section 3 we discuss discrimination between tops and stops through spin correlation. In section 4 the rapidity gap and its practical use are discussed. (In Appendix A we briefly show how these tools can be combined to achieve better sensitivity.) Finally in Sec. 5 we conclude.

2. Current LHC Searches

Several existing LHC studies have some bearing on the question of light stops, and will become increasingly applicable with more data. In this section, we will survey them, arguing that currently the main discriminating variables being used are the top cross section, missing E_T, and more sophisticated proxies for missing E_T (like transverse mass).

Because kinematics in the stealth regime resembles SM $t\bar{t}$ production, measurements of the top quark cross section potentially constrain stop production. One difficulty with attempting to find new physics simply by measuring the top cross section relative to its Standard Model value is that systematic uncertainties matter. As the top quark pole mass varies by about 5 GeV, the total cross section for $t\bar{t}$ production varies by about 15% [49]. In order to make a convincing measurement of new physics, then, one needs both an accurate measurement of the total cross section and an accurate kinematic measurement of the top pole mass. Furthermore, the theoretical prediction of cross section given mass must be accurate enough to resolve a discrepancy. Current theoretical calculations of cross sections have 10% errors from a combination of scale variation, α_s, and PDF uncertainties [46, 49]. Measurements of the top mass from kinematics can be fraught with difficulties over the precise definition of "top mass," with a common claim being that experiments have traditionally measured the ill-defined Pythia mass rather than the pole mass. Even the pole mass of the top is not well-defined, requiring a specification of the treatment of IR ambiguities due to confinement in QCD [50]. Inferences of the top quark pole mass from total cross section (using NNLO theory calculations [51]) at D$\varnothing$ [52], CMS [53], and ATLAS [54] yield $167.5^{+5.4}_{-4.9}$, $170.3^{+7.3}_{-6.7}$, and $166.4^{+7.8}_{-7.3}$ GeV, while the latest Tevatron combination for the top mass inferred from kinematics is 173.2 ± 0.9 GeV. A CMS cross section combination measured 165.8 ± 2.2 (stat.) $\pm$ 10.6 (syst.) $\pm$ 7.8 (lumi.) pb [55], whereas an ATLAS cross section combination measured 177 ± 3 (stat.)$^{+8}_{-7}$ (syst.) $\pm$ 7 (lumi.) pb [56]. Taking all of this into account, it is clear that any apparent 15% deviation in the top cross section would be much more plausibly attributed to uncertainties in α_s, PDFs, m_t, luminosity, or any

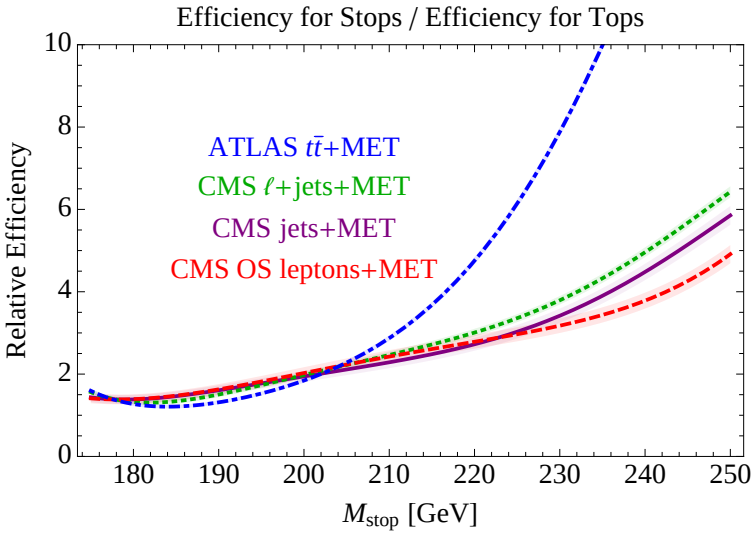

Figure 4: Estimated relative efficiency of various existing studies for tops and for stops decaying to (on- or off-shell) top and massless bino. Notice that efficiencies for stops do not become significantly larger than for tops until the stop mass is above about 210 GeV; the regime below this is the especially challenging case of stealthy stops. At higher masses, stops are easier to separate from tops, although rates become small. (At 210 GeV, the Prospino estimate shown in Figure 3 is $\sigma_{\rm stop} \approx 0.06\sigma_{\rm top}$.)

number of other systematic sources than to new physics. A claim of stop discovery *must* rely on kinematic and angular distributions, not simply rates.

Stops could also be constrained by various new physics searches, although these currently set weak limits, as discussed in [8, 9, 10]. We have computed the efficiency for stop pair production events to pass the cuts of some of the existing searches, and plotted its ratio to the efficiency for SM $t\bar{t}$ events in Figure 4 as a function of the stop mass. (The simulation makes use of Pythia [57, 58] and FastJet [59, 60].) As representative examples, we have plotted the medium cuts of the CMS all-hadronic search [4], the $250-350$ $S_T^{\rm lep}$ bin of the CMS lepton projection analysis [61], the high-MET selection of the CMS opposite-sign dileptons analysis [62], and the ATLAS $t\bar{t}+\not{\rm E}_{\rm T}$ analysis [63]. The estimate of the reach from these searches presented in [8] showed a possible limit near the top mass from the CMS $\ell+{\rm jets}+\not{\rm E}_{\rm T}$ search [61], and a hope for future exclusions above 250 GeV from the ATLAS $t\bar{t}+\not{\rm E}_{\rm T}$ search [63]. Moreover, the estimates of [9] showed a borderline exclusion of a single stop with a mass around 300 GeV by the ATLAS search [63]. The discrepancies in estimates between Refs. [8] and [9] are very minor and can possibly be explained by details of the simulation and finally resolved by an updated experimental search.

There are two interesting features to note in Figure 4. The first is that, for stops heavier than about 240 GeV, it is straightforward to build a search that has much higher efficiency for identifying stop events than top events. In particular, the ATLAS $t\bar{t}+\not{\rm E}_{\rm T}$ search does very well by focusing on the semileptonic channel and requiring a transverse mass cut $m_T(\ell, \not{\rm E}_{\rm T}) > 150$ GeV. For semileptonic top events, one expects this transverse mass variable to be dominated by the neutrino from a W decay and typically bounded

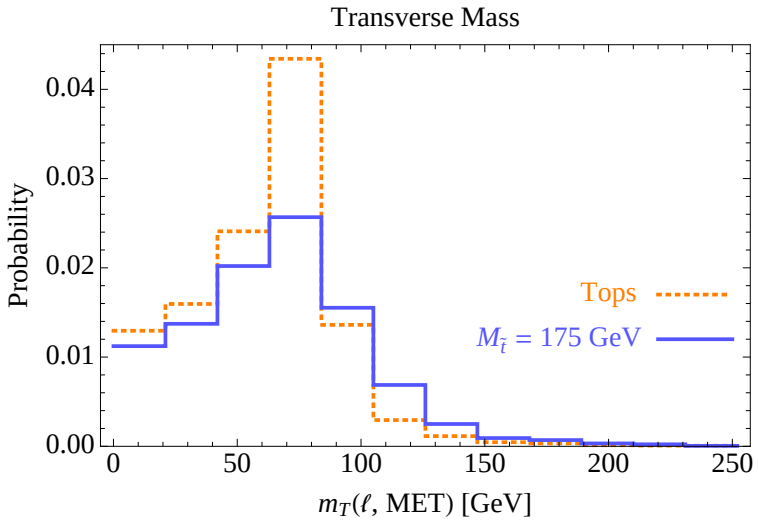

Figure 5: Fraction of events with transverse mass m_T in a given range and passing jet and lepton selection criteria from the ATLAS $t\bar{t}+$MET study [63]. Notice that stop events have a larger tail above M_W than top events do, even though the stop mass is barely above the top mass. This is due to three body decays $\tilde{t} \to bW^+\tilde{\chi}_1^0$. In the large m_T bins, the efficiency for stops is about twice the efficiency of tops.

above by 80 GeV. A significant background from dileptonic top events where one lepton is lost remains, but this too can be rejected by a clever variation on M_{T2} [30]. Similarly, one could search in the dileptonic channel using M_{T2} constructed with two leptons and missing E_T to reject $t\bar{t}$ backgrounds, again because it has an edge at the W mass [37, 8]. Thus, the lesson to take away from the dramatic rise in the blue dot-dashed curve in Figure 4 is that cutting on kinematic variables that are bounded above in the background can be very effective, and generalizations of these variables will be an interesting tool to apply in the future.

The second feature of Figure 4 that is interesting is the stealth regime, roughly 175 GeV $< M_{\rm stop} <$ 220 GeV (the upper limit of this regime is somewhat subjective). One might have expected that in this regime, the efficiency for stops would be almost identical to that for tops. We see in the figure that this isn't true, even for $M_{\rm stop} <$ 180 GeV; the efficiency of the selection cuts for stops very near the top mass is about 30% to 60% higher than that for tops, depending on the precise stop mass and the study considered. The reason is that, in the stealth regime, the bulk of the kinematic distributions for tops and stops are similar but the tails can still be significantly different. All of the new physics searches we have plotted involve large missing E_T requirements, which are more easily satisfied in the stop events than top events. In particular, for stops barely above the top mass, we have checked that the enhancement of the stop efficiency with the ATLAS $t\bar{t}+$MET selection cuts is explained by events in which at least one stop decay is 3-body, with $m(bW) \ll m_t$, allowing the bino to carry away significantly more missing momentum than stealth kinematics would predict. The resulting difference in transverse

mass distributions is shown in Figure 5.[2] At higher stop masses, 3-body decays become less important, but tails of kinematic distributions in which the bino momenta are as large as possible play a key role in the enhanced efficiency. Similar results were presented for Tevatron searches in Fig. 9 of Ref. [14], which focused on the gravitino case in which even more 3-body decays are present and the stop to top ratio can be even higher near the top mass. The lesson is that even in the stealth regime, missing E_T variables, especially clean ones like M_T or M_{T2} that can be designed to have edges in the background, can still play a useful role in constraining stops. However, 30% to 60% gains in S/B when starting with a signal an order of magnitude below the background leave much to be desired. A further difficulty is that, at these low masses, stop events will contaminate control regions of many studies, making it more difficult to infer the presence of a signal. We expect that in this regime missing energy variables are best used as part of a larger toolkit that exploits other differences in top and stop kinematics. In the rest of the paper, we will aim to build that toolkit.

Before continuing, let us make a simple estimate of the number of events that we can expect to be able to work with. With 20 fb^{-1} and an NLO $t\bar{t}$ rate of about 200 pb, and estimating a typical selection efficiency of about 20%, we expect to have (ignoring taus) about 40,000 dileptonic top events, 200,000 semileptonic top events, and 350,000 all-hadronic events. In this paper we will concentrate on signals with leptons, to avoid the potentially large QCD backgrounds in the all-hadronic channel. Note that if we knew the dileptonic top rate perfectly, a sample of 4,000 stops on top of 40,000 tops would have $S/\sqrt{B} \sim 20$. Of course, in reality systematic uncertainties overwhelm a simple cut-and-count method, but this number shows that our task is not hopeless, provided we can find shape variables with convincing differences.

3. Spin Correlations

3.1 Spin correlation

In the SM tops, being fermions, are pair produced with correlated polarizations that manifest in certain measurable angular variables [64, 65, 66, 67, 68, 69, 70]. For instance, at the LHC, where top production is dominated by $gg \to t\bar{t}$, when one top is left-handed the other tends to be as well, and similarly for the right-handed case (see Ref. [71] for an overview, and [72] for a study in the context of new physics). However, tops produced via stop decays have no such correlation because the scalar stops can not preserve any spin information. Therefore we can take advantage of techniques that were previously developed to measure spin correlation in $t\bar{t}$ pairs. In our case the goal is much more challenging. We do not compare the hypothesis that the top and antitop have Standard Model spin correlation with the hypothesis that they are completely uncorrelated, but rather with the

[2]The spill-out of $t\bar{t}$ events beyond $m_T(\ell, \not{E}_T) = m_W$ is caused by dileptonic events (with one lepton being lost) or by events with a τ (either leptonic or hadronic). Another possible source of these events can possibly be detector smearing, which is not captured here, since we do not run detector simulation. We expect that the latter effect is minor.

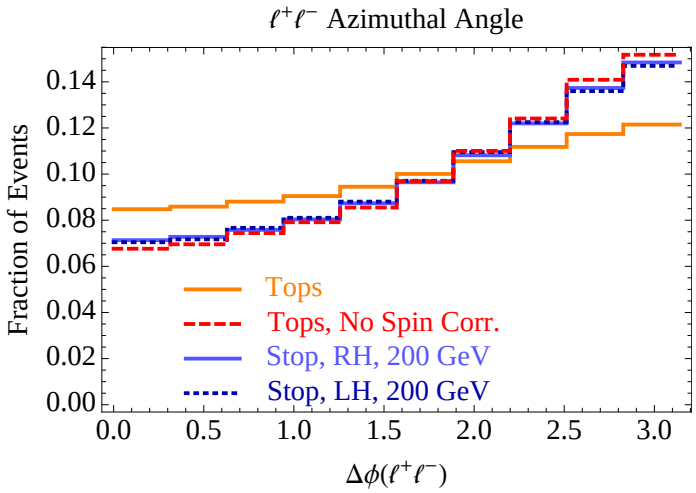

Figure 6: $\Delta\phi(\ell^+, \ell^-)$ for $t\bar{t}$ production, $\tilde{t}\tilde{t}^*$ production, and $t\bar{t}$ production with spin correlation turned off (i.e., the differential rates for production and decay are factorized and we randomize the top helicities in between). Notice that, from the point of view of this variable, stops are essentially the same as spin-uncorrelated tops. Also, polarization effects are small, as left- and right-handed stops have the same distribution.

hypothesis that a spin-correlated $t\bar{t}$ sample has $\mathcal{O}(10\%)$ contamination from scalar events, which approximately look like spin-uncorrelated tops.[3]

When the LSPs are soft, stop events are similar to top pair events without correlation. This is illustrated in Figure 6, which shows one distribution, $\Delta\phi(\ell^+, \ell^-)$, which is sensitive to spin correlations, and for which stops look like tops with spin correlation turned off. We have calculated the observable for tops with MC@NLO [75, 76] at parton level, and checked that corrections from varying the top mass and the renormalization and factorization scales are small relative to the shift that would arise from adding a sample of stops to the tops. This observable has been studied by ATLAS to probe the existence of spin correlations in $t\bar{t}$ production [77], with the most recent update achieving 5σ significance for the existence of nonzero correlation effects [78].

In order to confirm the SM top pair spin correlation Ref. [48] proposed a method using full matrix elements with and without spin correlation. This method has been implemented experimentally in Tevatron searches [79, 80], which observed evidence for spin correlation in both the dileptonic and semileptonic channels. Since many more top events are produced at the LHC than at the Tevatron, we are expecting a more precise measurement at the LHC of the $t\bar{t}$ spin correlation. Any deviation from the SM prediction will be a sign of new physics. In the presence of light stops, we will observe a mixture of correlated and uncorrelated top pairs. In the following, we discuss the use of the matrix element method in stop searches. We concentrate on the dileptonic channel in the following discussion.

[3] One other effect that could play a role in angular distributions turns out to be unimportant for us: the stop can be mostly right-handed or mostly left-handed (as some theoretical models predict; see e.g. [24]), and so the tops coming from the stop decays can be polarized. While it can be an appreciable effect if the mass splitting between top and stop is large [73, 74], it is a small effect in the stealthy regime, as we have checked explicitly. Hence, we will not discuss it further.

We have also checked the semileptonic channel, which gives a less significant effect due to combinatorial uncertainties.

For a dedicated stop search, it would be optimal to use directly the stop matrix element, which involves both the matrix element for the $2 \to 2$ process and the one for subsequent particle decays. However, as we will discuss further in Section 4, the differential cross section for the $2 \to 2$ process is subject to large theoretical uncertainties. On the other hand, it was observed in Ref. [48] that the spin correlation information for $t\bar{t}$ production is stable against NLO corrections at the LHC. Therefore, it is illuminating to examine the spin correlation alone, without invoking explicitly the stop pair matrix element. For this purpose, we use the matrix elements for top pairs with and without correlations, as they were given in [70]. (The spin uncorrelated matrix element was derived from the assumption that top decays are completely spherically symmetric in the rest frame of the top). This is also a generic approach that allows us to find signs of new physics in $t\bar{t}$ correlations without specifying the underlying theory.

3.2 Implementation in stop searches

In the dileptonic channel, we reconstruct the events and calculate the likelihood distributions as follows. Top and stop events are generated at parton level (including spin correlations) with MadGraph [41] and showered with Pythia [57, 58]. Jets are clustered with FastJet using the anti-k_T algorithm with radius 0.4 [59, 60], and we apply simple isolation requirements to define leptons, which are identical to the isolation criteria of [81].

1. Events are required to pass the following kinematic cuts, which closely follow (but are not identical to) the event selection used by ATLAS in Ref. [81].

   - At least two jets with $p_T > 25$ GeV and $|\eta| < 2.5$, one or two of which must be b-tagged.
   - Two opposite-sign leptons with $p_T > 20$ GeV and $|\eta| < 2.5$.
   - In the e^+e^- and $\mu^+\mu^-$ channels, the invariant mass of the two leptons must satisfy $m_{\ell\ell} > 15$ GeV and $|m_{\ell\ell} - M_Z| < 10$ GeV. In addition we demand $\not{E}_{\rm T} > 40$ GeV.
   - In the $e\mu$ channel, no cut is applied on $m_{\ell\ell}$ or $\not{E}_{\rm T}$. Instead, a cut on H_T (defined as the scalar sum of all selected charged leptons and jets) is applied: $H_T > 130$ GeV.

2. We apply a flat b-tagging efficiency of 65% (this is conservative relative to the 80% quoted in Ref. [81]). For events with only one b-jet, we consider all non-b jets with $p_T > 25$ GeV as a candidate for the other b-jet. Then for each combination of two b-jets and two leptons, we can use the W and top mass shell constraints to solve for the momenta of the two neutrinos from W decays, assuming they are the only missing particles in the event. There could be 0, 2 or 4 real solutions. We discard events without real solutions. The final efficiency is 16.8% for tops and 15.6% for stops. All

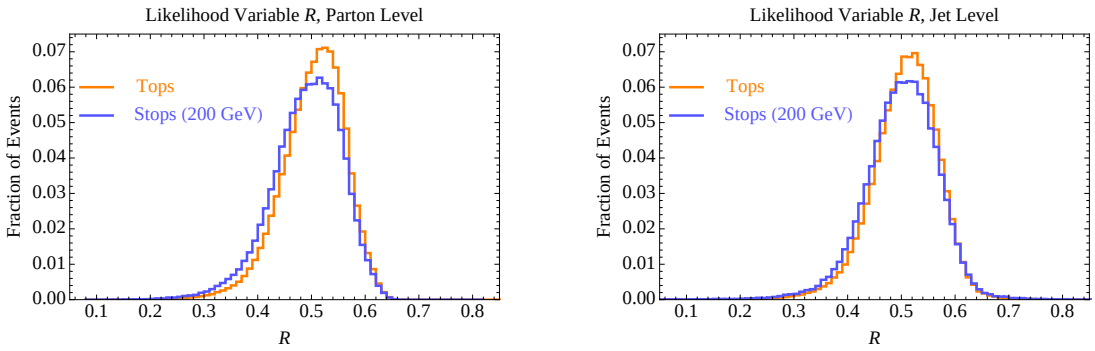

Figure 7: The likelihood variable $\mathcal{R}$. Left: parton level; right: jet level.

solutions from all combinations are taken into account in the following calculation. Following Ref. [48], we define the probability distribution for a given event as

$$P_H = \mathcal{N}_H^{-1} \sum_{ij} \sum_a J_a f_i^{(a)} f_j^{(a)} \left| \mathcal{M}_H^{ij} \left(p_{\rm obs}, p_\nu^{(a)}, p_{\bar{\nu}}^{(a)} \right) \right|^2 , \tag{3.1}$$

where $H = \{\text{corr,uncorr}\}$ denotes the hypothesis of correlated or uncorrelated tops, $\mathcal{N}_H$ is a normalization factor, J_a is the Jacobian which appears when integrating over the neutrino momenta, f_i and f_j are the parton distribution functions for the two incoming partons, and $\mathcal{M}_H^{ij}$ is the leading order matrix element. The sum over a is the sum of all combinations and solutions. The sum over i, j is over all possible initial partons, gg, $u\bar{u}$ and $d\bar{d}$. For each event, we calculate both $P_{\rm corr}$ and $P_{\rm uncorr}$ and define the variable $\mathcal{R}$ as

$$\mathcal{R} = \frac{P_{\rm corr}}{P_{\rm corr} + P_{\rm uncorr}}. \tag{3.2}$$

The variable $\mathcal{R}$ is the likelihood for an event to be a correlated top pair. The $\mathcal{R}$ distributions for top event and stop events are shown in Fig. 7. For comparison, we also show the $\mathcal{R}$ distribution at the parton level.

3. Given the $\mathcal{R}$ distributions, we can also follow Ref. [48] to calculate the log likelihood ratio L to discriminate between two hypotheses with a set of N events. Here, L is defined as

$$L = 2\ln(\mathcal{L}_t/\mathcal{L}_{\tilde{t}}), \tag{3.3}$$

where

$$\mathcal{L}_\mathcal{K} \equiv \prod_i^N \rho_K(\mathcal{R}_i) \tag{3.4}$$

and $\rho_K(\mathcal{R}_i)$ is the probability density read from Fig. 7. we choose the number of top pair events corresponding to 20 fb^{-1} at 8TeV and compare it with the same number of events, but with top and stop mixed in the ratio of 12:1, corresponding to the

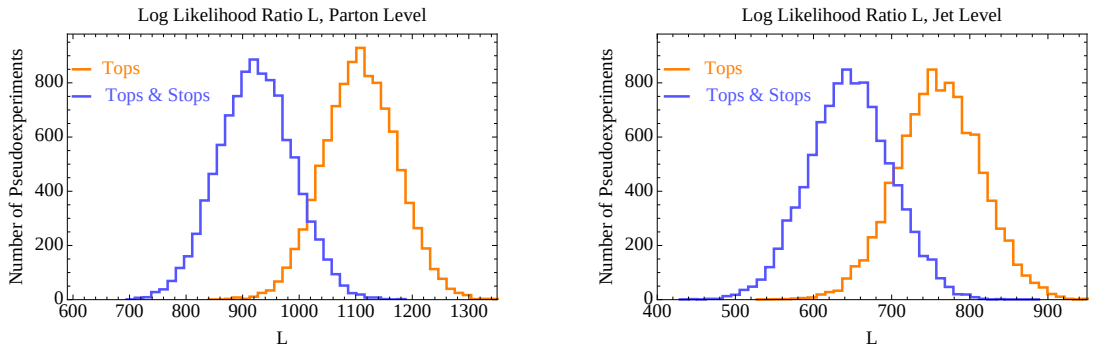

Figure 8: The log likelihood ratio L. Each point on the curve corresponds to a pseudoexperiment with 32.8k events. Note in particular that each top plus stop pseudoexperiment is normalized to the same number of events as each top pseudoexperiment. Left: parton level; right: jet level.

ratio in the cross sections. After kinematic cuts and reconstruction, we are left with 32.8k top events for the pure samples, and 30.4k top events and 2.4k stop events for the mixed sample. We generate 10k pseudo-experiments corresponding to the two cases and the resulting L distributions are shown in Fig. 8. For comparison, we also generate 10k pseudo-experiments at the parton level using the same number of events as the jet level (after reconstruction). From the jet level result in Fig. 8, we estimate that on average a light stop of 200 GeV can be excluded at 95% confidence level.

4. Rapidity Gaps

4.1 Top and stop production amplitudes

Initial state	$t\bar{t}$	$\tilde{t}\tilde{t}^*$
gg	68 pb	11 pb
$q\bar{q}$	23 pb	1.6 pb

Table 2: LO cross sections for top and stop production processes in MadGraph, for a 180 GeV stop. Notice, in particular, the tininess of stop production from $q\bar{q}$ due to the p-wave threshold, as well as the significant suppression of stop relative to top production even from gluons.

As illustrated in Figure 3, the pair production rate of stops, even with a mass equal to the top mass, is well below the pair production rate of tops. Delving into the differences in stop and top production processes will shed some light on this, and also suggest a set of variables that can be useful in discriminating top from stop events. The rates for top and stop production at leading order, from either $q\bar{q}$ or gg initial states, are shown in Table 2. The most striking fact is the smallness of $q\bar{q} \to \tilde{t}\tilde{t}^*$, which is explained by p-wave suppression: the stops in the final state need to carry angular momentum. Since they have no spin, this implies that they are produced in a p-wave with a rate $\propto \beta^3$ near threshold.

However, no such simple argument explains the ratio between stop and top production initiated by gluons. Naively, we might expect that the top and stop are both color triplets, so that for energies far above threshold, their production rates will be identical up to factors counting degrees of freedom, so that the rate for stops is asymptotically half that of tops. Table 2 makes it clear that this misses some aspect of the physics.

We can get some insight by considering the behavior of the differential cross section in the massless limit. For stops, there is a well-defined total rate [47]:

$$\sigma(gg \to \tilde{t}_1 \tilde{t}_1^*) \to_{s \gg m} \frac{5\alpha_s^2 \pi}{48 s}, \tag{4.1}$$

On the other hand, for massless quarks, one has [82]:

$$\frac{d\sigma}{d\Omega}(gg \to q\bar{q}) = \frac{\alpha_s^2}{24 s}\left(t^2 + u^2\right)\left(\frac{1}{tu} - \frac{9}{4s^2}\right), \tag{4.2}$$

which doesn't have a well-defined integral over phase space due to the t- and u-channel poles. Because the top is massive, we expect that this integral will be regulated and that the result will be a $\log \frac{s}{m_t^2}$ enhancement in the rate for forward top production in the parton center-of-momentum frame. This is a very real physical difference between the production of top quarks and scalar top quarks, which we should try to exploit. It is easy to see by considering the even simpler case of scalar QED versus QED, where the simplest MHV amplitudes with the right little group properties are easily written down and give the correct answers:

$$A^{\text{tree}}(1^+, 2^-, 3_\phi, 4_\phi) = ie^2 \frac{[1\ 3]\,\langle 2\ 3\rangle}{\langle 1\ 3\rangle\,[2\ 3]} = e^2 \times \text{ phase} \tag{4.3}$$

$$A^{\text{tree}}(1^+, 2^-, 3^-_{\bar{\psi}}, 4^+_{\psi}) = ie^2 \frac{[1\ 4]\,\langle 2\ 3\rangle}{\langle 1\ 3\rangle\,[2\ 3]} = e^2 \sqrt{\frac{u}{t}} \times \text{ phase}. \tag{4.4}$$

The latter case corresponds to the familiar splitting function ameliorating the pole in a t-channel diagram to the square root of a pole in the amplitude. In the scalar case, this pole is completely absent. The two results are, in fact, related by a SUSY Ward identity.

4.2 Parton-level distributions and systematics

Our intuition from the limits of massless particles is useless if it does not carry over to a fact about physical, massive tops and stops, but it does. The distribution of rapidity gaps between produced tops and stops is shown in Figure 9. The distributions are clearly different. However, we should keep in mind the fundamental fact about stop rates: in a sample of candidate top events, we are usually looking for at most 10% of the sample composed of stops, so even a 50% difference in the shape of pure top and stop distributions will become a 5% effect in the combined sample. We must investigate the robustness of our Monte Carlo predictions of the shape of the top rapidity gap distribution, to understand whether such an effect can ever be measured. We will begin by assessing this at parton level, ignoring subtleties associate with jets and detectors. Making the case that the difference is observable at this level is a necessary but not sufficient precondition for claiming that it can be measured at the LHC.

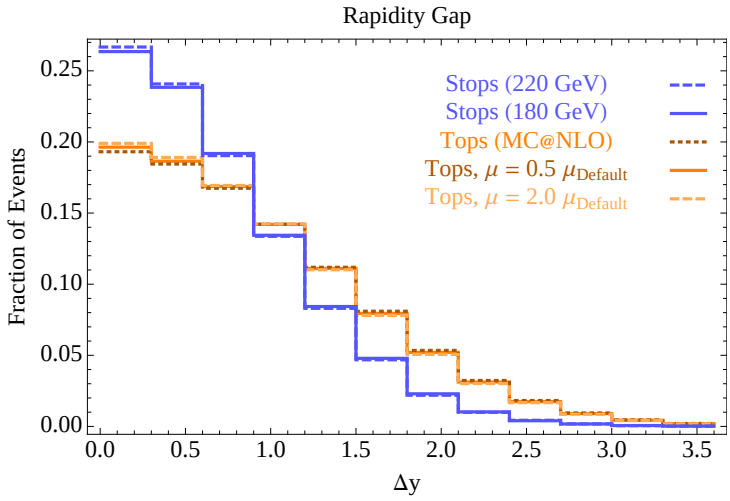

Figure 9: Δy distribution between top and antitop for $t\bar{t}$ production (orange) and for a 180 GeV scalar top (blue), both normalized to 1. Stops are more likely to be produced at small rapidity difference because the t- and u-channel poles in fermionic quark production from gg are absent in scalar quark production. Three curves are shown for tops, corresponding to different choices of renormalization and factorization scales in MC@NLO.

We have generated large samples of $t\bar{t}$ events using MC@NLO [75, 76] to assess the systematic uncertainties. We have varied both the factorization and renormalization scales, and the top quark mass, to analyze the effects on the shape of the Δy distribution. The fractional change in shape, bin-by-bin, is plotted in Figure 10. Here we have computed the binned Δy shape for different scale choices, normalized the shapes to unit area, and given the size of the shift in each bin relative to MC@NLO with default choices. We do not show variations of the top mass in the plot because we found the shape to be insensitive to it. We also show in Figure 10 the change in the default shape from tops when 12% of the sample is composed of 180 GeV stops instead of tops. Although the shape change can be significant, we see that much of the effect can be mimicked by increasing the renormalization scale. This compares only the *shape*, not the normalization. Doubling the renormalization scale also lowers the cross section by about 13%, whereas the presence of 180 GeV stops increases it by about 12%. However, the lowered cross section can be compensated to some extent if the top mass is lower, and the total top rate has at least a 10% theoretical uncertainty, as we reviewed in Section 2. The bottom line is that the rapidity distribution carries definite physical information, but to use it we must be cautious about systematic uncertainties in our understanding of top quark production. Continuing progress in understanding of tops at NNLO [83] could play a role in reducing these uncertainties.

Parton distribution functions could also be a source of uncertainty. We have not systematically explored this, but as one illustrative example, switching MC@NLO's choice of PDF set from the default CTEQ 6M to an Alekhin NLO FFN set produced a curve similar to the $\mu = 0.5\ \mu_{\rm Default}$ curve in Figure 10. Understanding PDF uncertainties would clearly be one component of getting Standard Model $t\bar{t}$ predictions under enough control to make statements about the presence of new physics with any confidence.

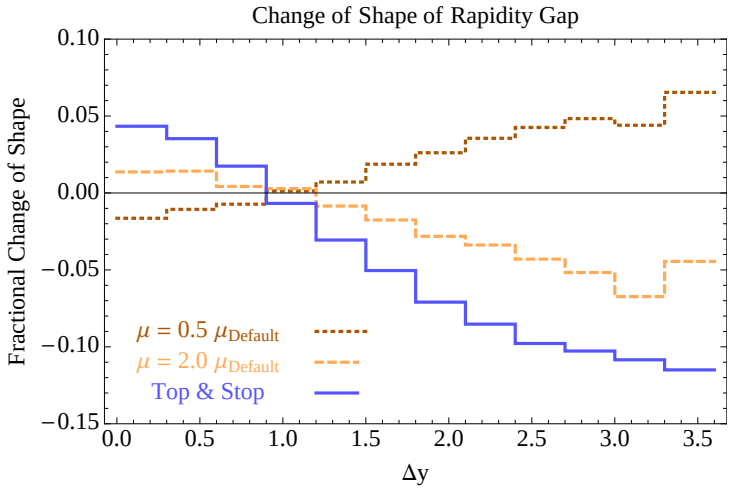

Figure 10: Relative fractional change in the fraction of events in each bin of Δy. The comparison is to MC@NLO run with default renormalization and factorization scales. The dotted dark orange curve is the result of halving these scales. The dashed light orange curve doubles the scales. The blue curve is the result of adding an admixture of 180 GeV stops (12% of the events, based on the relative NLO cross sections). The concern is that the effect of stops may be mimicked by a larger renormalization scale.

So far we have been discussing only inclusive parton-level quantities. Cuts on kinematic variables can help to draw out the differences between stops and tops. In Figure 9, both stops and tops peak at $\Delta y = 0$. This is because both are dominantly produced near threshold, where one has $\Delta y = 0$ by definition. In fact, one can easily see that as a function of the center-of-mass energy of the parton collision, $\sqrt{\hat{s}}$, there is a bound on Δy in $t\bar{t}$ events:

$$\Delta y \leq \log \frac{\hat{s} + \sqrt{\hat{s} - 4m_t^2}}{\hat{s} - \sqrt{\hat{s} - 4m_t^2}} \tag{4.5}$$

The same consideration applies to the $t\bar{t}$ subsystem of a stop event. Figure 11 shows where events lie in the plane of $(M_{t\bar{t}}, \Delta y)$; tops are seen to prefer larger Δy at larger $M_{t\bar{t}}$. This is not surprising since the t-/u-channel singularity is regularized by m_t, and as $\hat{s}$ grows, tops approaches a massless quark limit. Thus, a cut on $\hat{s}$ will allow us to isolate the regime where there *can*, in principle, be large differences between top and stop events. However, there is a caveat: a hard cut on $\hat{s}$ will make the difference in distributions clear, but runs the risk of diluting our samples enough that statistical uncertainties overwhelm the systematics and prevent us from drawing a clean conclusion.

As the bottom right-hand plot of Figure 11 shows, the mass cut also does not eliminate the systematic uncertainty: varying the factorization and renormalization scales upward by a factor of 2 continues to mimic much of the effect of adding stops to the top sample. It may be that a variable can be constructed that will capture similar physics while reducing systematic uncertainties. We have studied the Collins-Soper angle, which corrects the angle of the top quark to the beam direction to minimize the effects of ISR [84], as one possibility, but found that it was not an improvement.

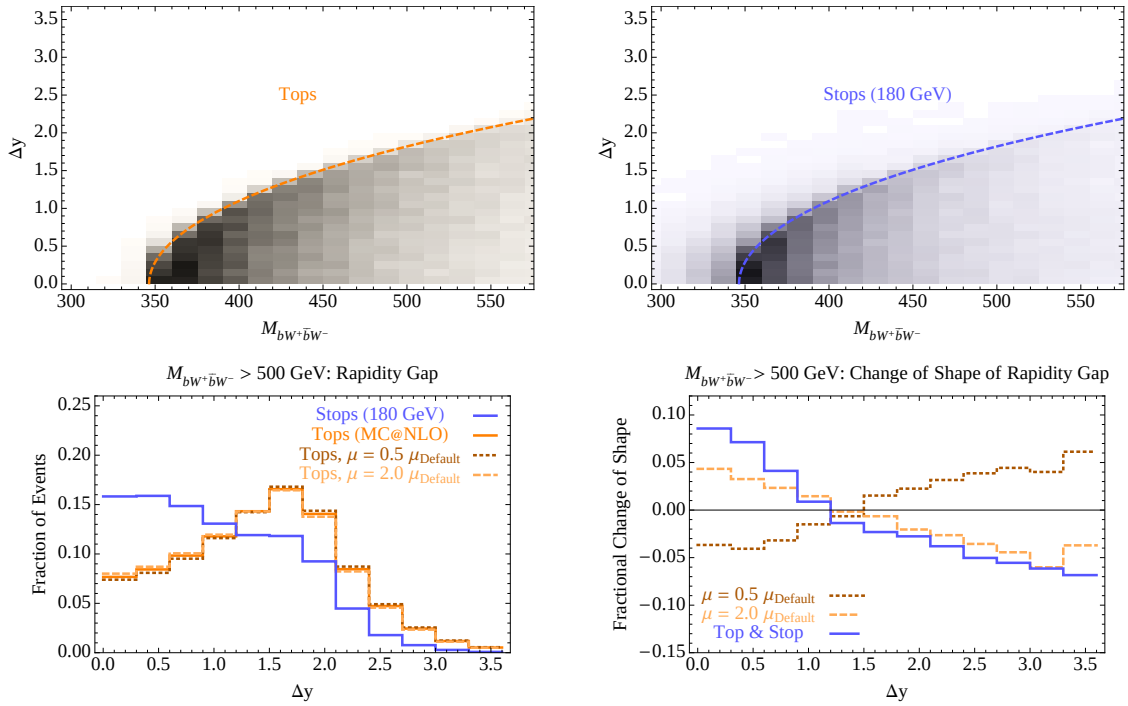

Figure 11: Top: correlation between the $t\bar{t}$ invariant mass (which for tops characterizes the center-of-mass energy $\sqrt{\hat{s}}$ of the parton collision) and the value of Δy. Notice that at larger $M_{t\bar{t}}$, the tops are more strongly peaked at larger Δy than the stops. The dashed curves correspond to Eq. 4.5; some stop events spill over the line, because the decays are off-shell (in which case we have replaced p_{top} with $p_b + p_W$ in the definitions of $M_{t\bar{t}}$ and Δy). **Bottom**: the analogues of Figures 9 and 10 after imposing a cut $M_{t\bar{t}} > 500$ GeV. The mass cut leads to a more dramatic shape difference, but the systematic effect of varying the renormalization and factorization scales can still mimic the signal.

4.3 Jet-level distributions and practical use

In spite of the systematic uncertainties discussed in the previous subsection, it can be useful to exploit the rapidity gap as one more variable that can potentially discriminate between a pure top sample and a stop-enriched one. The most straightforward way would be reconstructing the entire event and using the rapidity gap between the tops. Although possible, we find that this approach is not ideal. It is clear that some stop events, where the neutralinos contribute an appreciable portion of the $\not{E}_{\text{T}}$, will not pass reconstruction criteria. In this way, we lose the most pronounced non-top-like events. Nonetheless, applying the same reconstruction as in Section 3, we find $2\,\sigma$ significance from $\Delta y(t, \bar{t})$ alone. (The combination with spin correlations is discussed in Appendix A.)

To avoid this undesired loss of valuable events, we find another variable which is closely tied to the rapidity gap between the tops. It turns out that the rapidity gap between the leptons in the dileptonic events closely follows the rapidity gap between the tops. The rapidity gap between the leptons also grows in a $t\bar{t}$ sample as $m_{t\bar{t}}$ increases.

We also do not use the top invariant mass in our study, because it would force us

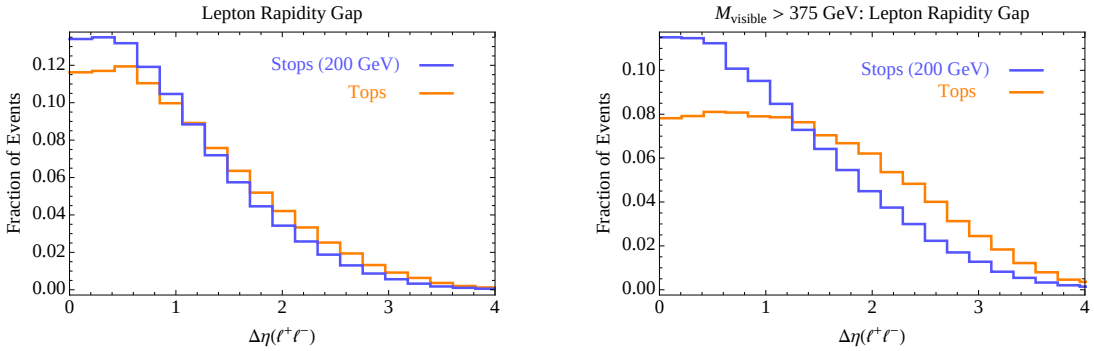

Figure 12: Rapidity gap distribution for tops and stops, normalized to the rate of events passing the cuts. The distribution on the LH side includes all the events which pass simple $t\bar{t}$ acceptance cuts. The distribution on the right shows only those events which have a visible mass higher than 375 GeV, as explained in the text.

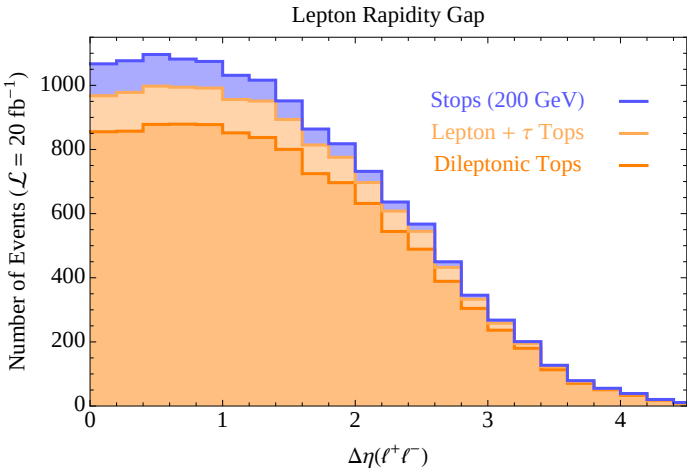

Figure 13: Rapidity gap between the leptons after the cut on the "visible mass" as explained in the text.

again to reconstruct the event. One might also consider reconstructing the invariant mass of *all* the objects in the event but this would introduce an undesired sensitivity to the ISR/FSR, deteriorating the correlation with $m_{t\bar{t}}$. Instead we choose a different quantity which closely mimics the behavior of the invariant mass and can be easily calculated without full event reconstruction. This quantity is an invariant mass of the leading visible objects in a dileptonic $t\bar{t}$ event. If both b-jets are tagged, we simply construct an invariant mass of two leptons and two b-jets. If only one b-jet is tagged, we construct an invariant mass of the leptons, b-jet and the non-tagged jet with the highest p_T in the event.

We illustrate our approach in Fig. 12. To build these plots we select the following events (these selection criteria are very similar to [85, 81]):

- Events with precisely two isolated leptons. The p_T of each lepton must exceed 20

GeV and $|\eta_l| < 2.5$.[4]

- Each event should have two or more jets, $p_T(j) > 25$ GeV, $|\eta(j)| < 3.0$.
- At least one jet should be b-tagged; we assume a flat tagging rate of 65%.
- $\not{E}_{\rm T} > 35$ GeV
- Discard the events with OSSF leptons and invariant mass 76 GeV $< m_{ll} <$ 106 GeV (Z-window)
- In the second sample we demand the invariant mass of the leading visible objects as explained before to be higher than 375 GeV.

We also plot in Fig. 13 an event distribution in a mixed top-stop sample and compare it to pure top. Notice that our cuts slightly favor stops. The acceptance for stops is 26.5%, while the acceptance for tops is 25.5%. This happens because the stop sample tends to have slightly higher $\not{E}_{\rm T}$ than tops, even though this tendency is not sufficient to discriminate between them alone. This is the feature we illustrated early in the paper in Fig. 1. Note that the excess of events in in the bins with $|\Delta\eta| < 1$ exceeds 10%, and maybe in combination with other distributions can be a good variable to discover or exclude the light stop.

Finally we briefly discuss (lack of) contamination of these samples with other backgrounds. First, one might worry about $(Z \to \tau_\ell \tau_\ell) + jj$, but it was shown in [85] that this background becomes negligible when two or more jets are required. The second important background is dileptonic DY production with jets. In this background the missing E_T usually comes from mismeasurement. It was also shown in [85] that a modest cut on $\not{E}_{\rm T} > 35$ GeV and the requirement of two jets render this background subdominant. Although this search was performed for $\sqrt{s} = 7$ TeV, there is no reason to believe that the results of a $\sqrt{s} = 8$ TeV search will be very different. Hence, have we neglected these backgrounds throughout the paper.

5. Discussion

Naturalness could still manifest itself through a variety of possible signatures. A heavy stop, for instance, could decay to a lighter stop to produce $t\bar{t}Z + \not{E}_{\rm T}$ [88]. The sbottom provides its own novel and possibly easier-to-find signatures [89, 90, 91, 92]. Higgsinos must be light for tree-level naturalness, and if they are the LSP or NLSP they can lead to more easily-observed stop decays [10, 93, 94]. Furthermore, deviations in Higgs boson production and decay rates from the Standard Model could also provide hints that naturalness is at work. Simultaneous pursuit of all of these signatures is necessary for a complete picture.

Here we have focused on the "stealth stop" regime in which missing momentum is relatively small, and argued that rapidity gap and spin correlation observables can help to

[4] Even softer isolated muons were allowed in the search [85], if they were the softest lepton in the event, so in this sense our results can be further improved.

build the case for a new physics signal. For less stealthy stops, we expect variants on missing E_T (especially transverse mass variables and their generalizations, which are bounded in $t\bar{t}$ background) to be relatively successful at digging stop signals out of top backgrounds. Even in that case, however, we would emphasize that the rapidity gap and spin correlation observables are diagnostic of the production of scalar particles. They may be less essential for discovering a signal, but could play a key role in establishing the nature of the signal. In particular, the distinct rapidity distributions of stops as opposed to fermionic top partners gives a new handle on spin determination. These measurements could be made with the next year's worth of data, and so we eagerly await the LHC's verdict on light stops.

Acknowledgments

We thank Lisa Randall for collaboration in the early stages of this project. We thank Rick Cavanaugh, Kirill Melnikov, Jessie Shelton, Matt Schwartz, and Brock Tweedie for useful discussions. ZH is supported in part by NSF grant PHY-0804450. AK is supported by NSF grant PHY-0855591. MR is supported by the Fundamental Laws Initiative of the Harvard Center for the Fundamental Laws of Nature. DK and MR thank the New Physics @ Korea Institute and the Shilla Seoul for hosting a productive workshop where a portion of this work was completed. The computations in this paper were run on the Odyssey cluster supported by the FAS Sciences Division Research Computing Group at Harvard University.

A. Multivariate Analyses

We have seen that there are various differences in distributions in top and stop events that can be understood on physical grounds, mostly related to the angular momentum properties of the final states. Although one could try to construct a stop search using any one of them, or using various cuts designed to enhance signal to background, we expect that the most flexible and powerful approach is a multivariate analysis that uses all of the information. First, we would like to check that the variables we have used so far are not highly correlated.

One way to check for correlations is to bin one variable and plot the other; we take this approach in Figure 14, which shows that selecting particular ranges of $\Delta\phi(\ell^+, \ell^-)$ makes relatively minor changes in the shape of the $\Delta y(t, \bar{t})$ distribution. Another check is to compare the two-dimensional distribution of simulated points in the $(\Delta y, \Delta\phi)$ plane with the product of two one-dimensional distributions. Comparing binned samples of $t\bar{t}$ events (10 bins in $\Delta\phi$ by 12 bins in Δy), we find that in any given bin, the ratio of the two-dimensional probability to the product of the two one-dimensional probabilities is always in the range 0.92 to 1.08. Hence, we expect that the discussions in Sec. 3 and Sec. 4 are approximately orthogonal, and we can achieve better significance by combining the two approaches. (Of course, one would want to be sure systematic uncertainties on Δy are under control before taking this approach too seriously.)

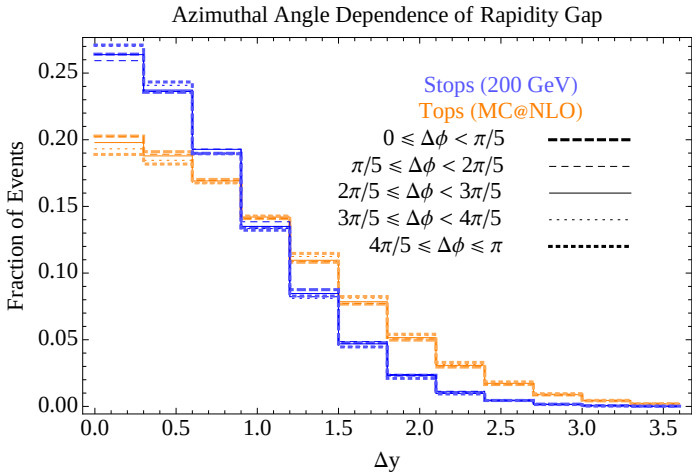

Figure 14: Rapidity gap between top and antitop, as in Figure 9, with the samples binned based on $\Delta\phi(\ell^+, \ell^-)$. We see that the distributions are not strongly correlated, in the sense that restricting to a subset of $\Delta\phi$ values makes little difference in the shape of the $\Delta y(t, \bar{t})$ curve.

Along these lines, we consider a simple multivariate method by taking the product of probabilities defined from one dimensional distributions [95, 96]. For a given variable x, we obtain the signal and background distributions in two histograms with the same binning and normalized to the same area. Then we define the probability of an event in bin i being a signal event as

$$p_s^x = \frac{n_s^i}{n_s^i + n_b^i}. \tag{A.1}$$

Correspondingly, the event has a probability $(1 - p_s^x)$ being a background event. For multiple variables, the total probability is defined as

$$\mathcal{P}_s = \frac{\prod_x p_s^x}{\prod_x p_s^x + \prod_x (1 - p_s^x)}. \tag{A.2}$$

Then we can treat $\mathcal{P}_s$ as a single variable and repeat the likelihood test as in Sec. 3 for the two hypotheses and obtain the L distributions. In Fig. 15, we show the L distributions by combining the spin correlation variable $\mathcal{R}$ and the reconstructed rapidity gap $\Delta y(t\bar{t})$, for 20 fb^{-1} data. The reconstruction procedure is the same as in Sec. 3. Note that in this approach, the correlations among different variables are not taken into account. Nonetheless, as for the $(\Delta y, \Delta\phi)$ distributions, the correlations between the two variables are small. Therefore we obtain significantly better discriminating power than using each individual variable: the two distributions are separated by $\sim 3\sigma$ in Fig. 15, while the two variables alone each give us $\sim 2\sigma$ significance.

B. Boosted Stops

As discussed in Sec. 2, while measurements of the top production rate are in principle sensitive to stop production, difficulties arise because of challenging systematic uncertainties.

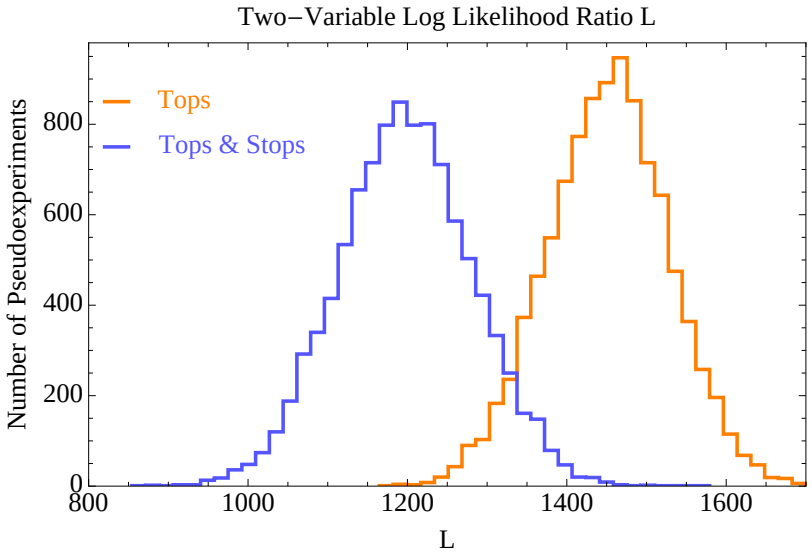

Figure 15: The log likelihood ratio L by combining two variables: R and $\Delta y_{t\bar{t}}$. Each point on the curve corresponds to a pseudoexperiment with 32.8k events.

Indeed, even at NNLL theoretical uncertainties in the top cross section are comparable to the size of the contributions we expect from stops.

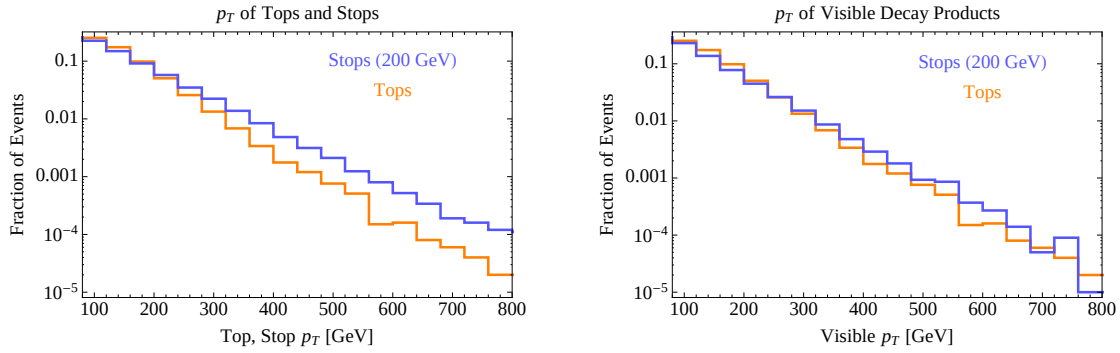

Figure 16: Parton-level p_T distributions of tops and stops (left) and of the corresponding visible decay products (right). These distributions are normalized so that the top and stop share the same inclusive rate. Note that here we have taken $m_{\tilde{t}} = 200$ GeV.

However, the physics which suppresses the stop production rate relative to that of tops (*i.e.* phase space suppression from the larger stop mass, p-wave suppression, and the absence of t and u-channel poles - see Sec. 4) tends to have a diminished effect at higher p_T's. This can be seen by comparing normalized stop/top p_T distributions, as shown on the left hand side of Fig. 16. One might therefore expect that through the use of top-tagging techniques (see Ref. [97] and references contained therein) one could observe a significant increase in top production at high p_T coming from the decay of boosted stops.

Alas, this is not the case for the stealth region we have considered. The distribution

of top/stop p_T's is steeply falling, and at high boosts the transverse momentum carried away by the LSP is enough to shift the distribution in p_T of the visible decay products downward enough to largely cancel any hoped-for benefits (the fractional change in p_T is roughly $\Delta m_{\tilde{t},t}/m_t$). See the right-hand side of Fig. 16. For this reason we do not include a more detailed study of boosted stops, although they can be useful outside of the stealthy regime.

References

[1] S. Dimopoulos and G. Giudice, *Naturalness constraints in supersymmetric theories with nonuniversal soft terms*, *Phys.Lett.* **B357** (1995) 573–578, [hep-ph/9507282].

[2] A. G. Cohen, D. Kaplan, and A. Nelson, *The More minimal supersymmetric standard model*, *Phys.Lett.* **B388** (1996) 588–598, [hep-ph/9607394].

[3] **ATLAS** Collaboration, G. Aad *et al.*, *Search for squarks and gluinos using final states with jets and missing transverse momentum with the ATLAS detector in* $\sqrt{s} = 7$ *TeV proton-proton collisions*, 1109.6572.

[4] **CMS** Collaboration, *Search for supersymmetry in all-hadronic events with missing energy*, CMS-PAS-SUS-11-004, 2011.

[5] **ATLAS** Collaboration, *Search for squarks and gluinos using final states with jets and missing transverse momentum with the atlas detector in* $\sqrt{s}$ *= 7 tev proton-proton collisions*, ATLAS-CONF-2012-033, CERN, Geneva, Mar, 2012.

[6] **CMS** Collaboration, *Search for new physics in the multijets + missing transverse energy final state in 7 tev proton-proton collisions*, CMS-PAS-SUS-12-011, 2012.

[7] R. Essig, E. Izaguirre, J. Kaplan, and J. G. Wacker, *Heavy Flavor Simplified Models at the LHC*, *JHEP* **1201** (2012) 074, [1110.6443].

[8] Y. Kats, P. Meade, M. Reece, and D. Shih, *The Status of GMSB After 1/fb at the LHC*, *JHEP* **1202** (2012) 115, [1110.6444].

[9] C. Brust, A. Katz, S. Lawrence, and R. Sundrum, *SUSY, the Third Generation and the LHC*, *JHEP* **1203** (2012) 103, [1110.6670].

[10] M. Papucci, J. T. Ruderman, and A. Weiler, *Natural SUSY Endures*, 1110.6926.

[11] X.-J. Bi, Q.-S. Yan, and P.-F. Yin, *Probing Light Stop Pairs at the LHC*, 1111.2250.

[12] N. Desai and B. Mukhopadhyaya, *Constraints on supersymmetry with light third family from LHC data*, 1111.2830.

[13] **ATLAS** Collaboration, *Search for scalar bottom pair production with the ATLAS detector in pp Collisions at sqrts = 7 TeV*, 1112.3832.

[14] Y. Kats and D. Shih, *Light Stop NLSPs at the Tevatron and LHC*, *JHEP* **1108** (2011) 049, [1106.0030].

[15] **ATLAS** Collaboration, *Search for gluinos in events with two same sign leptons, jets and missing transverse momentum*, ATLAS-CONF-2012-004, CERN, Geneva, Feb, 2012.

[16] **CMS** Collaboration, S. Chatrchyan *et al.*, *Search for new physics in events with same-sign dileptons and b-tagged jets in pp collisions at sqrt(s) = 7 TeV*, 1205.3933.

[17] **CMS** Collaboration, *Search for supersymmetry in events with a single lepton and jets using templates*, CMS-PAS-SUS-11-027, CERN, Geneva, Aug, 2011.

[18] **ATLAS** Collaboration, *Hunt for new phenomena using large jet multiplicities and missing transverse momentum with ATLAS in* $L = 4.7\ fb^{-1}$ *of* $\sqrt{s} = 7\ TeV$ *proton-proton collisions*, ATLAS-CONF-12-037.

[19] R. Sundrum, *SUSY Splits, But Then Returns*, *JHEP* **1101** (2011) 062, [0909.5430].

[20] R. Barbieri, E. Bertuzzo, M. Farina, P. Lodone, and D. Pappadopulo, *A Non Standard Supersymmetric Spectrum*, *JHEP* **1008** (2010) 024, [1004.2256].

[21] M. Redi and B. Gripaios, *Partially Supersymmetric Composite Higgs Models*, *JHEP* **1008** (2010) 116, [1004.5114].

[22] N. Craig, D. Green, and A. Katz, *(De)Constructing a Natural and Flavorful Supersymmetric Standard Model*, *JHEP* **1107** (2011) 045, [1103.3708].

[23] C. Csaki, Y. Shirman, and J. Terning, *A Seiberg Dual for the MSSM: Partially Composite W and Z*, *Phys.Rev.* **D84** (2011) 095011, [1106.3074].

[24] C. Csaki, L. Randall, and J. Terning, *Light Stops from Seiberg Duality*, 1201.1293.

[25] N. Craig, M. McCullough, and J. Thaler, *Flavor Mediation Delivers Natural SUSY*, 1203.1622.

[26] P. Meade and M. Reece, *Top partners at the LHC: Spin and mass measurement*, *Phys.Rev.* **D74** (2006) 015010, [hep-ph/0601124].

[27] T. Han, R. Mahbubani, D. G. Walker, and L.-T. Wang, *Top Quark Pair plus Large Missing Energy at the LHC*, *JHEP* **0905** (2009) 117, [0803.3820].

[28] T. Plehn, M. Spannowsky, M. Takeuchi, and D. Zerwas, *Stop Reconstruction with Tagged Tops*, *JHEP* **1010** (2010) 078, [1006.2833].

[29] T. Plehn, M. Spannowsky, and M. Takeuchi, *Boosted Semileptonic Tops in Stop Decays*, *JHEP* **1105** (2011) 135, [1102.0557].

[30] Y. Bai, H.-C. Cheng, J. Gallicchio, and J. Gu, *Stop the Top Background of the Stop Search*, 1203.4813.

[31] N. Bhattacharyya, A. Choudhury and A. Datta, *Low mass neutralino dark matter in mSUGRA and more general models in the light of LHC data*, Phys. Rev. D **84**, 095006 (2011) arXiv:1107.1997 [hep-ph].

[32] A. Choudhury and A. Datta, *Many faces of low mass neutralino dark matter in the unconstrained MSSM, LHC data and new signals*, JHEP **1206**, 006 (2012) arXiv:1203.4106 [hep-ph].

[33] G. Isidori and J. F. Kamenik, *Forward-Backward t tbar Asymmetry from Anomalous Stop Pair Production*, Phys. Lett. B **700**, 145 (2011) arXiv:1103.0016 [hep-ph].

[34] D. S. M. Alves, M. R. Buckley, P. J. Fox, J. D. Lykken and C. -T. Yu, *Stops and MET: the shape of things to come*, arXiv:1205.5805 [hep-ph].

[35] D. E. Kaplan, K. Rehermann and D. Stolarski, *Searching for Direct Stop Production in Hadronic Top Data at the LHC*, arXiv:1205.5816 [hep-ph].

[36] C.-L. Chou and M. E. Peskin, *Scalar top quark as the next-to-lightest supersymmetric particle*, *Phys.Rev.* **D61** (2000) 055004, [hep-ph/9909536].

[37] T. Cohen, E. Kuflik, and K. M. Zurek, *Extracting the Dark Matter Mass from Single Stage Cascade Decays at the LHC*, *JHEP* **1011** (2010) 008, [1003.2204].

[38] T. Plehn, M. Spannowsky, and M. Takeuchi, *Stop searches in 2012*, 1205.2696.

[39] J. Fan, M. Reece, and J. T. Ruderman, *Stealth Supersymmetry*, *JHEP* **1111** (2011) 012, [1105.5135].

[40] J. Fan, M. Reece, and J. T. Ruderman, *A Stealth Supersymmetry Sampler*, 1201.4875.

[41] J. Alwall, M. Herquet, F. Maltoni, O. Mattelaer, and T. Stelzer, *MadGraph 5 : Going Beyond*, *JHEP* **1106** (2011) 128, [1106.0522].

[42] M. Reece, "Stop NLSP to Goldstino in MadGraph 5." available on the web.

[43] C. Degrande, C. Duhr, B. Fuks, D. Grellscheid, O. Mattelaer, *et al.*, *UFO - The Universal FeynRules Output*, *Comput.Phys.Commun.* **183** (2012) 1201–1214, [1108.2040].

[44] K. Melnikov, A. Scharf, and M. Schulze, *Top quark pair production in association with a jet: QCD corrections and jet radiation in top quark decays*, 1111.4991.

[45] W. Beenakker, M. Kramer, T. Plehn, M. Spira, and P. Zerwas, *Stop production at hadron colliders*, *Nucl.Phys.* **B515** (1998) 3–14, [hep-ph/9710451].

[46] M. Cacciari, M. Czakon, M. L. Mangano, A. Mitov, and P. Nason, *Top-pair production at hadron colliders with next-to-next-to-leading logarithmic soft-gluon resummation*, *Phys.Lett.* **B710** (2012) 612–622, [1111.5869].

[47] W. Beenakker, S. Brensing, M. Kramer, A. Kulesza, E. Laenen, *et al.*, *Supersymmetric top and bottom squark production at hadron colliders*, *JHEP* **1008** (2010) 098, [1006.4771].

[48] K. Melnikov and M. Schulze, *Top quark spin correlations at the Tevatron and the LHC*, *Phys.Lett.* **B700** (2011) 17–20, [1103.2122].

[49] M. Beneke, P. Falgari, S. Klein, and C. Schwinn, *Hadronic top-quark pair production with NNLL threshold resummation*, *Nucl.Phys.* **B855** (2012) 695–741, [1109.1536].

[50] A. H. Hoang, A. Jain, I. Scimemi, and I. W. Stewart, *Infrared Renormalization Group Flow for Heavy Quark Masses*, *Phys.Rev.Lett.* **101** (2008) 151602, [0803.4214].

[51] U. Langenfeld, S. Moch, and P. Uwer, *Measuring the running top-quark mass*, *Phys.Rev.* **D80** (2009) 054009, [0906.5273].

[52] **D0** Collaboration, V. M. Abazov *et al.*, *Determination of the pole and MSbar masses of the top quark from the $t\bar{t}$ cross section*, *Phys.Lett.* **B703** (2011) 422–427, [1104.2887].

[53] **CMS** Collaboration, *Determination of the top quark mass from the ttbar cross section at sqrt(s) = 7 tev*, CMS-PAS-TOP-11-008, 2011.

[54] **ATLAS** Collaboration, *Determination of the top-quark mass from the ttbar cross section measurement in pp collisions at sqrt(s)=7 tev with the atlas detector*, ATLAS-CONF-2011-054, CERN, Geneva, Mar, 2011.

[55] **CMS** Collaboration, *Combination of top pair production cross section measurements*, CMS-PAS-TOP-11-024, 2011.

[56] **ATLAS** Collaboration, *Statistical combination of top quark pair production cross-section measurements using dilepton, single-lepton, and all-hadronic final states at* $\sqrt{s} = 7$ *tev with the atlas detector*, ATLAS-CONF-2012-024, CERN, Geneva, Mar, 2012.

[57] T. Sjostrand, S. Mrenna, and P. Z. Skands, *PYTHIA 6.4 Physics and Manual*, *JHEP* **0605** (2006) 026, [hep-ph/0603175].

[58] T. Sjostrand, S. Mrenna, and P. Z. Skands, *A Brief Introduction to PYTHIA 8.1*, *Comput.Phys.Commun.* **178** (2008) 852–867, [0710.3820].

[59] M. Cacciari and G. P. Salam, *Dispelling the* N^3 *myth for the* k_t *jet-finder*, *Phys.Lett.* **B641** (2006) 57–61, [hep-ph/0512210].

[60] M. Cacciari, G. P. Salam, and G. Soyez, *FastJet user manual*, 1111.6097. See also M. Cacciari, G.P. Salam, and G. Soyez, FastJet.

[61] **CMS** Collaboration, *Search for new physics with single-leptons at the lhc*, CMS-PAS-SUS-11-015, 2011.

[62] **CMS** Collaboration, *Search for new physics in events with opposite-sign dileptons and missing transverse energy*, CMS-PAS-SUS-11-011, 2011.

[63] **ATLAS** Collaboration, G. Aad *et al.*, *Search for New Phenomena in ttbar Events With Large Missing Transverse Momentum in Proton-Proton Collisions at sqrt(s) = 7 TeV with the ATLAS Detector*, *Phys.Rev.Lett.* **108** (2012) 041805, [1109.4725].

[64] M. Jezabek and J. H. Kuhn, *Lepton Spectra from Heavy Quark Decay*, *Nucl.Phys.* **B320** (1989) 20.

[65] T. Stelzer and S. Willenbrock, *Spin correlation in top quark production at hadron colliders*, *Phys.Lett.* **B374** (1996) 169–172, [hep-ph/9512292].

[66] G. Mahlon and S. J. Parke, *Maximizing spin correlations in top quark pair production at the Tevatron*, *Phys.Lett.* **B411** (1997) 173–179, [hep-ph/9706304].

[67] G. Mahlon and S. J. Parke, *Angular correlations in top quark pair production and decay at hadron colliders*, *Phys.Rev.* **D53** (1996) 4886–4896, [hep-ph/9512264].

[68] A. Brandenburg, *Spin spin correlations of top quark pairs at hadron colliders*, *Phys.Lett.* **B388** (1996) 626–632, [hep-ph/9603333].

[69] S. J. Parke and Y. Shadmi, *Spin correlations in top quark pair production at* e^+e^- *colliders*, *Phys.Lett.* **B387** (1996) 199–206, [hep-ph/9606419].

[70] G. Mahlon and S. J. Parke, *Spin Correlation Effects in Top Quark Pair Production at the LHC*, *Phys.Rev.* **D81** (2010) 074024, [1001.3422].

[71] S. J. Parke, *Spin Correlation Effects in Top Quark Pair Production*, 1005.0347.

[72] M. Baumgart and B. Tweedie, *Discriminating Top-Antitop Resonances using Azimuthal Decay Correlations*, JHEP **1109**, 049 (2011) 1104.2043.

[73] M. Perelstein and A. Weiler, *Polarized Tops from Stop Decays at the LHC*, *JHEP* **0903** (2009) 141, [0811.1024].

[74] J. Shelton, *Polarized tops from new physics: signals and observables*, Phys. Rev. D **79**, 014032 (2009), 0811.0569.

[75] S. Frixione and B. R. Webber, *Matching NLO QCD computations and parton shower simulations*, *JHEP* **0206** (2002) 029, [hep-ph/0204244].

[76] S. Frixione, P. Nason, and B. R. Webber, *Matching NLO QCD and parton showers in heavy flavor production*, *JHEP* **0308** (2003) 007, [hep-ph/0305252].

[77] **ATLAS** Collaboration, *Measurement of spin correlation in $t\bar{t}$ production from pp collisions at $\sqrt{s} = 7$ tev using the atlas detector*, ATLAS-CONF-2011-117, CERN, Geneva, Aug, 2011.

[78] G. Aad *et al.* [ATLAS Collaboration], *Observation of spin correlation in $t\bar{t}$ events from pp collisions at sqrt(s) = 7 TeV using the ATLAS detector*, Phys. Rev. Lett. **108**, 212001 (2012) arXiv:1203.4081 [hep-ex].

[79] **D0** Collaboration, V. M. Abazov *et al.*, *Measurement of spin correlation in $t\bar{t}$ production using a matrix element approach*, *Phys.Rev.Lett.* **107** (2011) 032001, [1104.5194]. 7 pages, 3 figures, submitted to Phys. Rev. Lett.

[80] **D0** Collaboration, V. M. Abazov *et al.*, *Evidence for spin correlation in $t\bar{t}$ production*, *Phys.Rev.Lett.* **108** (2012) 032004, [1110.4194]. 7 pages, 2 figures.

[81] **ATLAS** Collaboration, G. Aad *et al.*, *Measurement of the cross section for top-quark pair production in pp collisions at sqrt(s) = 7 TeV with the ATLAS detector using final states with two high-pt leptons*, 1202.4892.

[82] B. Combridge, J. Kripfganz, and J. Ranft, *Hadron Production at Large Transverse Momentum and QCD*, *Phys.Lett.* **B70** (1977) 234.

[83] P. Baernreuther, M. Czakon, and A. Mitov, *Percent level precision physics at the Tevatron: first genuine NNLO QCD corrections to $q\bar{q} \to t\bar{t} + X$*, 1204.5201.

[84] J. C. Collins and D. E. Soper, *Angular Distribution of Dileptons in High-Energy Hadron Collisions*, *Phys.Rev.* **D16** (1977) 2219.

[85] **CMS** Collaboration, *Top pair cross section in dileptons*, CMS-PAS-TOP-11-005, 2011.

[86] A. Barr, *Measuring slepton spin at the LHC*, *JHEP* **0602** (2006) 042, [hep-ph/0511115].

[87] A. Alves and O. Eboli, *Unravelling the sbottom spin at the CERN LHC*, *Phys.Rev.* **D75** (2007) 115013, [0704.0254].

[88] M. Perelstein and C. Spethmann, *A Collider signature of the supersymmetric golden region*, *JHEP* **0704** (2007) 070, [hep-ph/0702038].

[89] H. Li, W. Parker, Z. Si, and S. Su, *Sbottom Signature of the Supersymmetric Golden Region*, *Eur.Phys.J.* **C71** (2011) 1584, [1009.6042].

[90] A. Datta and S. Niyogi, *Entangled System of Squarks from the Third Generation at the Large Hadron Collider*, 1111.0200.

[91] H. M. Lee, V. Sanz, and M. Trott, *Hitting sbottom in natural SUSY*, 1204.0802.

[92] E. Alvarez and Y. Bai, *Reach the Bottom Line of the Sbottom Search*, 1204.5182.

[93] M. Asano, H. D. Kim, R. Kitano, and Y. Shimizu, *Natural Supersymmetry at the LHC*, *JHEP* **1012** (2010) 019, [1010.0692].

[94] **ATLAS** Collaboration, G. Aad *et al.*, *Search for scalar top quark pair production in natural gauge mediated supersymmetry models with the ATLAS detector in pp collisions at sqrt(s) = 7 TeV*, 1204.6736.

[95] **CDF** Collaboration, T. Aaltonen *et al.*, *Observation of Single Top Quark Production and Measurement of —Vtb— with CDF*, *Phys.Rev.* **D82** (2010) 112005, [1004.1181].

[96] Y. Bai and Z. Han, *Improving the Top Quark Forward-Backward Asymmetry Measurement at the LHC*, *JHEP* **1202** (2012) 135, [1106.5071].

[97] T. Plehn and M. Spannowsky, *Top Tagging*, 1112.4441.